International Journal of Modern Physics E
© World Scientific Publishing Company

arXiv:1510.02591v1 [nucl-ex] 9 Oct 2015

A Study of Fluctuations of Voids in Relativistic Ion-Ion Collisions

SHAKEEL AHMAD, M.M. KHAN, SHAISTA KHAN, A. KHATUN AND M. IRFAN

Department of Physics, Aligarh Muslim University
Aligarh 202002, India
sa_hep@yahoo.com

Received (received date)
Revised (revised date)

Event-by-event fluctuations of hadronic patterns are investigated in terms of voids by analyzing the experimental data on 4.5, 14.5 and 60A GeV/c ^{16}O-AgBr collisions. The findings are compared with the predictions of a multi-phase transport AMPT model. Dependence of voids on phase space bin width is examined in terms of two lowest moments of event-by-event fluctuations of voids, $< G_q >$ and S_q. The findings reveal that scaling exponent estimated from the observed power-law behavior of the voids may be used to characterize the various properties of hadronic phase transition. The results also rule out occurrence of 2^{nd} order quark-hadron phase transition at the projectile energies considered.

1. Introduction

One of the main goals of studying relativistic nucleus-nucleus (AA) collisions is to investigate characteristics of strongly interacting matter under extreme conditions of initial energy density and/or temperature, where formation of quark-gluon-plasma (QGP) is envisaged to take place[1,2,3]. Fluctuations in physical observables of these collisions are regarded as one of the important signals of QGP formation because of the fact that in many body systems phase transition may cause significant changes in quantum fluctuations of an observable from its average behavior[1,3]. Furthermore, presence of large fluctuations in event-by-event (ebe) analysis may indicate existence of distinct classes of events, one with and one without QGP formation[4,5] Fluctuations in physical observables are essentially of two types: the ones arising due to finite multiplicity are referred to as the statistical fluctuations.These fluctuations can be filtered out by considering independent emission of particles. All other fluctuations are of dynamical origin and are known as 'dynamical' fluctuations[4]. Dynamical fluctuations can be divided into two groups: (i) fluctuations which do not change on ebe basis such as two-particle correlations due to Bose Einstein statistics or due to decays of resonances and (ii) fluctuations exhibiting ebe variation, generally called ebe fluctuations.Examples are: fluctuations in the ratio of charged to neutral particle multiplicities due to creation of Disoriented Chiral Condensates (DCC) and occurrence of jets may contribute to the ebe fluctuations[4].

A system undergoing a second order phase transition is envisaged to exhibit large fluctuations and long-range correlations[6]. If the symmetry of the quark system created in a heavy-ion collisions is such that the quark-hadron phase transition is of the second order then large fluctuations are expected in the multiplicity of hadrons not only from event-to-event but also from one region to the other in the geometrical space in which emission of hadrons takes place[6]. Such local hadron density fluctuations would result in the formation of spatial patterns involving cluster of hadrons and regions of no hadrons between adjacent clusters[6,7]. The non-hadronic regions between the clusters, termed as voids, may, therefore, provide a significant insight into the fluctuations associated with the critical behavior of QGP phase transition[7]. Hwa and Zhang[8] have proposed a method to investigate fluctuations of spatial patterns in terms of voids. It may be revealed that only a few attempts[7,9] have been made to study fluctuations of voids in hadronic and ion-ion collisions at high energies. It was, therefore, considered worthwhile to undertake a systematic study of fluctuations of voids by analyzing the experimental data on AA collisions at different incident energies. This would help identify some baseline contributions to the fluctuations of voids.

2. Method of Analysis

As mentioned earlier, a method of analyzing fluctuations of voids has been recently proposed by Hwa and Zhang[8]. Detailed description about this method are presented in refs.7,9. However, a brief description about the method of analysis requires attention hence discussed here. It may be interesting to mention that single particle density distribution in pseudorapidity (η) space is non-flat. In order to have a flat distribution, following new cumulative variable, X(η) has been introduced[10,11,12]:

$$X(\eta) = \frac{\int_{\eta_{min}}^{\eta} \rho(\eta) d(\eta)}{\int_{\eta_{min}}^{\eta_{max}} \rho(\eta) d(\eta)} \tag{1}$$

where η_{min} and η_{max} denote respectively the minimum and maximum values of η-range considered, whereas $\rho(\eta)$ represents single particle rapidity density. Thus, X(η) is uniformly distributed between 0 and 1. The one-dimensional X(η) space is divided into M bins of equal width, $\delta(= 1/\mathrm{M})$. The multiplicity of relativistic charged particles produced in each event will vary from bin to bin. There will be bins with a few or more hadrons and also with no hadron et al. The bins with no hadron(s) are termed as the empty bins. If two or more empty bins are adjacent, these bins are cumulatively added and treated as a single void[7]. If there are one or more non-empty bins present between two empty bins, then these are considered as separate voids. The size of a void is simply the number of empty bins connected to one another. Shown in Fig.1 is a typical pattern of voids in a configuration generated for M = 16. The open squares represent empty bins, while the filled ones indicate the non-empty bins. Let V_k denote the sum of the empty bins connected

then the fraction of bins that kth void occupies is defined as[7,9];

$$x_k = V_k/M \tag{2}$$

Thus, for each event there is a set $S_e(= x_1, x_2, x_3....)$ of void fractions that characterizes the spatial pattern. Since the pattern fluctuates from event to event, S_e can not,therefore, be used for comparing patterns in an efficient way. For comparison, Hwa and Zhang[8] have defined a moment g_q for each configuration as;

$$g_q = \frac{1}{m}\sum_{k=1}^{m} {x_k}^q \tag{3}$$

where, the sum is over all voids in an event, m represents the total number of voids while q is the order of the moment. The normalized G moments of order q are defined as[8]

$$G_q = \frac{g_q}{g_1^q} \tag{4}$$

which depend not only on q but also on M. Thus, by definition $G_0 = G_1 = 1$. It should be mentioned that G_q having above definition are quite different from those used in studying the erraticity of rapidity gaps[8,11,13] because x_k do not satisfy the sum rule. The G_q are also different from G moments used in the study of multifractality[14]. G_q given by Eq.(4) is a number for every event for a given set of values of q and M. For a fixed q and M, G_q would exhibit fluctuations in its values from event to event and is a measure of the void patterns.
The ebe fluctuations of G_q can be examined by plotting the probability distribution, $P(G_q)$, for a given set of events. Using such a probability distribution, several moments may be calculated. The two lowest moments are[8,9];

$$< G_q >= \frac{1}{N_{ev}}\sum_{e=1}^{N_{ev}} G_q^{(e)} \tag{5}$$

and

$$S_q =< G_q ln G_q > \tag{6}$$

where, the superscript 'e' denotes the eth event and N$_{ev}$ is the number of events in a data sample. The two moments, $< G_q >$ and S_q, are expected to obey power-law behavior as;

$$< G_q > \propto M^{\gamma_q} \tag{7}$$

$$S_q \propto M^{\sigma_q} \tag{8}$$

Such a scaling behaviour implies that voids of all sizes occur at phase transition. since the moments corresponding to different q are highly correlated, the scaling exponents γ_q and σ_q are expected to depend on q in the following fashion:

$$\gamma_q = c_0 + cq \tag{9}$$

$$\sigma_q = s_0 + sq \tag{10}$$

Thus, the values of c and s, which represents the slopes of slopes are concise characterization of the fluctuations near the critical point.

3. Experimental Details

Three samples of events produced in the interactions of 4.5, 14.5 and 60A GeV/c ^{16}O beams with AgBr group of nuclei in emulsion are used in the present study. These events are taken from the emulsion experiments performed by EMU01 Collaboration[15,16,17,18]. The events were searched for by along-the-track scanning method, which gives a relative minimum bias sample because of its inherent high detection efficiency[15,16,19,20]. The events lying within 2-5 cm from the edge of the pellicle were considered for various measurements[15,19]. The tracks of the secondary particles were identified on the basis of their ionization[15,16,20]. The tracks having ionization, $I < 1.4I_0$, where I_0 is the minimum ionization produced by a singly charged relativistic particle, are known as the shower tracks. The tracks having ionization in the range, $1.4I_0 \leq I \leq 10I_0$ are referred to as grey tracks, whereas those having ionization $I > 10I_0$ are termed as black tracks. The numbers of grey and black tracks produced in an event are denoted by n_g and n_b respectively. The grey and the black tracks are jointly called as heavily ionizing tracks and their number in an interaction is denoted by $n_h = (n_b + n_g)$. Events with $n_h \leq 7$ are regarded to be produced either due to interactions with H or CNO group of nuclei or due to the peripheral collisions with AgBr group of nuclei, whereas the events with $n_h \geq 8$ are exclusively due to the collisions with AgBr group of targets[16,19,21]. On the basis of these criteria, events produced in the interactions of ^{16}O ion with AgBr targets were selected for the present analysis. The numbers of 4.5, 14.5 and 60A GeV/c ^{16}O-AgBr collisions events turn out to be 1200, 370 and 422 respectively. It should be emphasized that the conventional emulsion technique has two main advantages over the other detectors: (i) its 4π solid angle coverage and (ii) emulsion data are free from biases due to full phase space coverage. However, in the case of other detectors, only a fraction of charged particles are recorded due to the limited acceptance cone. This not only reduces the charged particle multiplicity but also distorts some of the event characteristics, like particle density fluctuations[19,22]. In order to compare the results of the present study with those predicted by a multi phase transport (AMPT) model, matching numbers of events were simulated using the code, ampt-v1.21-v2.21[23]. The events are simulated by taking into account the percentage of interactions which occur in collisions of projectile with various targets in emulsion[18]. While generating the AMPT event samples, the values of impact parameter are so set that the mean multiplicities of the relativistic charged particles, $< n_s >$ turns out to be nearly equal to those obtained for the experimental data.

4. Results and Discussion

Values of pseudorapidities of the relativistic charged particles produced in each event lying in the range, $\Delta\eta(= \eta_c \pm 3.0)$, where η_c is the center of symmetry of the η distribution, are transformed into $X(\eta)$ using Eq.(1). The one dimensional $X(\eta)$ space is divided into M bins of equal width, $\delta(= 1/M)$. The presence of voids are searched for following the approach discussed above and the sizes of the voids are determined. Void fractions, x_k, g_q moments and normalized G_q moments are calculated using Eqs.2-4. The values of G_q for q = 2-5 are calculated by varying the number of bins, M, from 16 to 96 in steps of 8. Distributions of G_q moments for q = 2 and M = 16 & 64 for the experimental and AMPT data at the three incident energies are plotted in Figs.2,3. It may be noticed from these figures that G_q fluctuate from event to event and the fluctuations are rather more pronounced for higher number of phase space bins. It may be of interest to mention that the shapes of G_q distributions are satisfactorily reproduced by those obtained using AMPT event samples. Furthermore, it is evident from Figs.2 and 3 that mean value of G_q and the dispersion of G_q distribution vary with M, for a fixed q, and also with q, for a fixed M (not shown). This suggests that in order to look at simple regularities in the nature of fluctuations of G_q, M dependence of $< G_q >$ over all configurations must be looked into[8].

Variations of $ln < G_q >$ with lnM for various data sets are shown in Figs.4 and 5. It is seen from the figures that $ln < G_q >$ increases with lnM . The lines in the figures are due to the best fits to the data of the form:

$$ln < G_q >= a_1 + b_1 M + c_1 M^2 \tag{11}$$

Values of constants a_1, b_1, c_1, appearing in the above expression are listed in Table 1. Our results reveal that variations of $ln < G_q >$ with lnM are quadratic in nature for both real and AMPT data sets at the three incident energies. These results are somewhat different from those reported earlier[7] for 200A GeV/c ^{32}S-AgBr and 350 GeV/c π^--AgBr collisions. These workers have observed a linear increase of $ln < G_q >$ with lnM. Hwa and Zhang[8] have also suggested that G_q vs M plots on log-log scale should be linear. Data points for to M = 32 and above, displayed in Figs. 4 and 5, indicate also linear increase of $ln < G_q >$ with lnM and suggest a power-law behavior expressible by Eq.(7). The values of slopes γ_q obtained from the best fits to the data (for M $\geq$ 32) are presented in Table 2. It may be noted from the Table that the values of γ_q for the experimental data are slightly higher than those for the AMPT events. Such scaling behavior may be interpreted as indication of occurrence of voids of all sizes[8].

Since the G_q moments of various orders are highly correlated, the scaling exponent γ_q, appearing in Eq.(7) is expected to depend on q in some simple ways. In order to examine this, variations of γ_q with q for the various data sets are plotted in Fig.6. The straight lines in the figure represent the best fits to the data of the form, given by Eq.(9). The values of coefficient "c" occurring in Eq.(9) are listed in Table 3. It has been suggested[8] that Eq.(9) may be regarded as a convenient parameterization

of γ_q that allows to regard "c" as a numeric description of the scaling behavior of voids.

Distributions of G_q, shown in Figs.2 and 3 indicate that by studying the behavior of $< G_q >$ only a limited information about the distribution may be extracted. However, the shape of G_q distribution would characterize the nature of ebe fluctuations in the distribution. A moment which quantifies the degree of these fluctuations is expressed as;

$$C_{p,q} = \frac{1}{N}\sum_{e=1}^{N}(G_q^{(e)})^p = \int dG_q G_q^p P(G_q) \tag{12}$$

As $C_{1,q}(=< G_q >)$ provides no information about the extent of fluctuations but the derivative of $c_{p,q}$ at $p = 1$,

$$S_q = \frac{d}{dp}C_{p,q}\Big|_{p=1} =< G_q lnG_q > \tag{13}$$

is envisaged to yield maximum information regarding the ebe fluctuations

Variations of lnS_q with lnM for the real data at the three incident energies are displayed in Fig.7, while Fig.8 exhibits similar plots for the AMPT events. The lines in the figures are due to the best fits to the data of the following form:

$$lnS_q = a_2 + b_2 M + c_2 M^2 \tag{14}$$

The values of the constants a_2, b_2, c_2, estimated for various event samples, are presented in Table 4. These results indicate that the trend of increase of lnS_q with lnM may be nicely reproduced by a 2^{nd} order polynomial. However, like G_q, linear fits to the data points for $M \geq 32$, shown in Figs.7 and 8 are obtained to study the power-law behavior expressed by Eq.(8). The values of slopes σ_q are presented in Table 5. It is observed that the values of σ_q for the experimental data are somewhat higher than those obtained for the AMPT event samples. Dependence of σ_q on q is displayed in Fig.9. The straight lines in the figure are due to parameterization of Eq.(10). The values of the coefficient "s" are presented in Table 3. It may be noted from the table that the values of "s" for the real data are slightly higher than those for the AMPT events. It may also be noted from the table that the values of "c" and "s" increase with increasing beam energy. It should be mentioned that the values of "c" for the experimental data lie between 0.26 and 0.46, whereas the values of "s" lie in the range 0.23 and 0.38. The values of "c" and "s" in the case of 200A GeV/c ^{32}S-AgBr collisions have been reported[7] to be 0.56 ± 0.01 and 0.43 ± 0.02 respectively. As a quantitative signature of 2^{nd} order quark-hadron phase transition, the values of "c" and "s" are predicted[8] to lie in the ranges 0.75-0.96 and 0.7-0.9 respectively. The values of the two parameters obtained in the present study are much smaller than those predicted for the 2^{nd} order quark-hadron phase transition, suggesting that no such phase transition occurs at the energies considered in the present study.

The method of voids used in the present study is one of the several approaches for studying ebe fluctuations, e.g., normalized factorial moments[24],

multifractals[12,14], erraticity[11,25], k-order rapidity spacing [22] and transverse momentum spectra[26]. Furthermore, fluctuations in the conserved quantities like baryon number, strangeness, electric charge, etc., have emerged as new tools to estimate degree of equilibration and criticality of the measured systems[27,28]. Higher moments like variance, σ^2, skewness, S, kurtosis, k, etc, of conserved quantities such as net baryon, net charge and net strangeness multiplicity distributions are regarded as important tools to search for the QCD critical point at RHIC and LHC energies[29,30,31,32]. Dynamical development of cooling and hadronization of QGP are studied in a simple model envisaging critical fluctuations in the QGP to hadronic matter and a 1^{st} order transition in a small finite system[32]. Variations of skewness and kurtosis as functions of system's temperature and volume abundance of hadronic matter are predicted which can be investigated via a beam energy scan program using the data at RHIC energies. Non-statistical fluctuations of higher order moment singularities of net proton event distributions in Au-Au collisions in the energy range: $\sqrt{s_{NN}}$ =11.5-200 GeV have been studied in the framework of parton and hadron cascade model, PACIAE[29,30,31]. It has been observed[30,31] that the energy dependence of higher order moments of the net proton multiplicity distributions observed using STAR data are in fine agreement with the predictions of the model[30]. PACIAE model predictions relating to energy dependence of various moments of net proton multiplicity distributions are also observed to be in fine agreement with the experimental results obtained using pp data at RHIC and LHC energies[29].

A method to determine critical temperature, T_c, by analysing the RHIC data has been proposed[30,33]. By studying the variations of σ^2, S and k with beam energy and comparing the findings with the lattice calculation results, the value of T_c has been reported to be 175^{+1}_{-7} MeV. However, no evidence of singularity in the study of energy dependence(for a fixed centrality) and/or centrality dependence(at a given energy) has been reported[31]. In order to explore the QCD phase diagram, several attempts[34,35,36,37,38,39,40] have also been made by analyzing the experimental data on pp and AA collisions in the center-of-mass energy range, $\sqrt{s_{NN}} \sim$ 7.7-200 GeV; this will also help study the various interesting features of higher order moments of net proton multiplicity distributions. Although these investigations do not provide unambiguous information that S and k and the products $S\sigma$ and $k\sigma^2$ are sensitive to the quark-gluon-hadron phase transition or any potential QCD critical point[36,37], yet the findings help understand non QCD critical point physics effects in the observables such as effects of conservation(of electric charge, baryon number and strangeness number), finite size, decays of resonances and hadronic scattering. Moreover, from the results based on the observables a baseline may be disentangled for the observables in order to search for the critical point[38].

As already stated we have analyzed the experimental data collected using emulsion technique, where the charges can not be identified, study of net proton multiplicity distribution is not possible. We have, therefore, used the method of voids to study

the fluctuations on ebe basis. It may be remarked that this method is fairly suitable for such studies using the data at relatively lower energies, AGS and SPS, because multiplicities at these energies are generally low and hence probability of occurrence of voids in the available range of rapidity will be quite large. If the multiplicities of hadrons vary significantly from one region to the other in the geometrical phase space then it becomes important to capture fluctuations using a detector capable of covering full phase space. Emulsion technique is the most suitable and advantageous because it allows full phase space coverage. Thus, the results obtained in the present study may help construct a baseline to the fluctuations arising from non-QGP critical point physics.

5. Conclusions

Results of the present study encourage to draw the following important conclusions:

(1) G_q distributions for different number of phase space bin, M, reveal that G_q fluctuate from event to event and the fluctuations are more pronounced in the case of higher values of M.

(2) Trends of variations of $< G_q >$ and S_q with number of bins, M, (on log-log scales) are nicely reproduced by a 2^{nd} order polynomial. However, for higher values of M, these variations tend become linear. Such a linear dependence would indicate the presence of power-law behavior, which would indicate existence of voids of all sizes.

(3) Scaling exponents, γ_q and σ_q estimated from the power-law dependence of G_q and S_q on the order number q are observed to grow linearly. However, the slopes obtained from the plots of γ_q and σ_q as a function of plots are found to be relatively much smaller than those predicted envisaging quark-hadron phase transition.

(4) Various characteristics of fluctuations of voids for the experimental data are observed to be in fine agreement with those predicted by AMPT model.

References

1. S. Ahmad *et al.*, *Adv. in High Energy Phys.* **2013** (2013) 836071
2. M. Rybezynski, *J. Phys.* G **35** (2008) 104091.
3. E. V. Shuryak, *Phys. Rep.* C **61** (1980) 71.
4. S. A. Voloshin *et al.*, *Phys. Rev.* C **60** (1999) 024901.
5. M. Doring and V. Koch, *Acta Phys. Pol.* B **33** (2002) 1495.
6. R. C. Hwa, *Phys. Rev.* C **64** (2001) 054904.
7. M. Mondal *et al.*, Astropart. Phys. **55** (2014) 26.
8. R. C. Hwa and Q.H. Zhang, *Phys. Rev.* C **62** (2000) 05902.

9. D. Ghosh *et al.*, *Phys. of Particle and Nuclei Lett.* **12** (2015) 246.
10. A. Bialas and M. Gazdzicki, *Phys. Lett.* B **252** (1990) 483.
11. S. Ahmad *et al.*, *Acta Phys. Pol.* B **35** (2004) 1.
12. S. Ahmad *et al.*, *Chaos Solitions and Fractals* **42** (2009) 538.
13. R. C. Hwa and Q.H. Zhang, *Phys. Rev.* D **62** (2000) 014003.
14. R. C. Hwa, *Phys. Rev.* D **41** (1990) 1456.
15. EMU01 Coll. (M.I. Adamovich *et al.*), *J. Phys.* G **22** (1996) 1469.
16. EMU01 Coll. (M.I. Adamovich *et al.*), *Phys. Lett* B **227** (1989) 285.
17. EMU01 Coll. (M.I. Adamovich *et al.*), *Phys. Rev. Lett.* **65** (1990) 412.
18. EMU01 Coll. (M.I. Adamovich *et al.*), *Phys. Lett.* **201** (1988) 397.
19. S. Ahmad et al., *Phys.Scr.* **87** (2013) 045201.
20. S. Ahmad et al., *Int. J. Mod. Phys.* E **23** (2014) 1450065.
21. C. F. Powell *et al,*, *Study of Elementary particles by Photographic method* (Pergamon Press, Oxford, 1959) p.450.
22. M. L. Cherry et al.,*Acta Phys. Pol.* B **29** (1998) 2129.
23. Z. W. Lin et al., *Phys. Rev.* C **72** (2005) 064901.
24. A. Bialas and R. Peschanski, *Nucl. Phys.* B **273** (1986) 703.
25. R. C. Hwa, *Acta Phys. Pol.* B **27** (1996) 1789.
26. STAR Coll. (J.C. Rider et al.), *Nucl. Phys.* A **698** (2002) 611c.
27. STAR Coll. (L. Adamczyk et al.), *Phys. Rev.* C **92** (2015) 021901(R).
28. ALICE Coll. (S. Jena) *J. Phys.* Conf. Ser.**612** (2015) 012047.
29. A. Limphirat *et al.*, *Cent. Eur. J. Phys.* **10** (2012) 1388.
30. D. M. Zhou *et al.*, *Phys. Rev.* C **85** (2012) 064916.
31. D. M. Zhou *et al.*, *J. Phys.* G **41** (2014) 065103.
32. L.P. Csernai *et al.*, *Phys. Rev.* C **85** (2012) 068201.
33. S. Gupta *et al.*, *Serence* **332** (2011) 1525.
34. STAR Coll. (X. Lou), *Cent. Eur. J. Phys.* **10** (2012) 1372.
35. STAR Coll. (X. Lou), *Acta Phys. Pol.* B Proc. Supp.**5** (2012) 497.
36. T. J. Tarnowsky and G.D. Westfall, *Phys. Lett* B **724** (2013) 51.
37. STAR Coll. (M.M. Agarwal *et al.*), *Phys. Rev. Lett.* **105** (2010) 022302.
38. X. Lou *et al.*, *Nucl. Phys.* A **931** (2014) 808.
39. STAR Coll. (B. Mohanty), *J. Phys.* G **38** (2011) 124023.
40. STAR Coll. (X. Lou), arXiv:1503.02558v2[nucl-ex] .

Table 1: Values of a_1, b_1, c_1 appearing in Eq. (10).

	Energy (A GeV/c)	q	a_1	b_1	c_1
Expt.	4.5	2	-1.899 ± 0.073	1.039 ± 0.041	-0.108 ± 0.005
		3	-3.741 ± 0.120	2.109 ± 0.070	-0.209 ± 0.010
		4	-5.403 ± 0.166	3.144 ± 0.102	-0.299 ± 0.015
		5	-7.201 ± 0.228	4.298 ± 0.142	-0.403 ± 0.021
	14.5	2	-3.357 ± 0.210	1.675 ± 0.112	-0.179 ± 0.014
		3	-4.885 ± 0.315	2.486 ± 0.181	-0.237 ± 0.025
		4	-6.329 ± 0.425	3.305 ± 0.260	-0.286 ± 0.038
		5	-7.997 ± 0.569	4.292 ± 0.362	-0.352 ± 0.055
	60	2	-6.249 ± 0.310	2.893 ± 0.158	-0.313 ± 0.020
		3	-6.662 ± 0.444	3.0 ± 0.246	-0.278 ± 0.033
		4	-7.235 ± 0.595	3.234 ± 0.349	-0.242 ± 0.049
		5	-8.083 ± 0.768	3.643 ± 0.468	-0.221 ± 0.068
AMPT	4.5	2	-1.882 ± 0.061	1.027 ± 0.034	-0.109 ± 0.004
		3	-4.291 ± 0.112	2.4 ± 0.065	-0.253 ± 0.009
		4	-6.395 ± 0.149	3.662 ± 0.092	-0.375 ± 0.013
		5	-8.73 ± 0.196	5.095 ± 0.127	-0.517 ± 0.019
	14.5	2	-3.781 ± 0.219	1.851 ± 0.114	-0.201 ± 0.014
		3	-5.935 ± 0.358	2.945 ± 0.197	-0.297 ± 0.026
		4	-7.232 ± 0.511	3.637 ± 0.295	-0.334 ± 0.041
		5	-8.293 ± 0.703	4.262 ± 0.421	-0.357 ± 0.060
	60	2	-5.543 ± 0.287	2.529 ± 0.147	-0.269 ± 0.018
		3	-5.727 ± 0.404	2.574 ± 0.224	-0.233 ± 0.030
		4	-6.326 ± 0.551	2.893 ± 0.324	-0.224 ± 0.046
		5	-7.304 ± 0.741	3.477 ± 0.455	-0.245 ± 0.067

Table 2: Values of slopes γ_q appearing in Eq. (6) for various data sets at different energies.

		Energy (A GeV/c)		
Type of events	q	4.5	14.5	60
Expt.	2	0.180 ± 0.006	0.250 ± 0.013	0.317 ± 0.015
	3	0.420 ± 0.016	0.598 ± 0.037	0.754 ± 0.040
	4	0.689 ± 0.028	1.006 ± 0.071	1.238 ± 0.081
	5	0.980 ± 0.042	1.455 ± 0.113	1.734 ± 0.136
AMPT	2	0.160 ± 0.005	0.232 ± 0.010	0.307 ± 0.016
	3	0.368 ± 0.014	0.569 ± 0.030	0.666 ± 0.038
	4	0.599 ± 0.027	0.947 ± 0.062	1.095 ± 0.077
	5	0.847 ± 0.043	1.249 ± 0.106	1.486 ± 0.132

Table 3: Values of coefficients c and s estimated using Eqs. (8) and (9) respectively.

Energy	c		s	
(A GeV/c)	Expt.	AMPT	Expt.	AMPT
4.5	0.26±0.01	0.22±0.01	0.23±0.02	0.18±0.02
14.5	0.38±0.02	0.34±0.02	0.32±0.04	0.26±0.04
60	0.46±0.03	0.38±0.03	0.38±0.05	0.29±0.05

Table 4: Values of a_2, b_2, c_2 appearing in Eq.(10).

	Energy (A GeV/c)	q	a_2	b_2	c_2
Expt.	4.5	2	-10.979 ± 0.295	4.910 ± 0.015	-0.545 ± 0.021
		3	-11.580 ± 0.355	5.920 ± 0.920	-0.648 ± 0.026
		4	-12.346 ± 0.415	6.912 ± 0.235	-0.741 ± 0.032
		5	-13.265 ± 0.475	7.871 ± 0.275	-0.825 ± 0.038
	14.5	2	-12.574 ± 0.741	5.361 ± 0.396	-0.573 ± 0.052
		3	-13.333 ± 0.931	6.510 ± 0.514	-0.689 ± 0.070
		4	-14.367 ± 1.128	7.569 ± 0.640	-0.781 ± 0.089
		5	-15.382 ± 1.324	8.509 ± 0.766	-0.850 ± 0.108
	60	2	-13.832 ± 0.741	5.465 ± 0.396	-0.536 ± 0.052
		3	-14.276 ± 1.168	6.306 ± 0.641	-0.616 ± 0.008
		4	-15.014 ± 1.393	7.137 ± 0.787	-0.612 ± 0.108
		5	-15.692 ± 1.601	7.817 ± 0.924	-0.695 ± 0.129
AMPT	4.5	2	-10.303 ± 0.351	4.910 ± 0.185	-0.493 ± 0.029
		3	-11.589 ± 0.502	5.900 ± 0.270	-0.650 ± 0.035
		4	-13.751 ± 0.696	7.611 ± 0.386	-0.841 ± 0.051
		5	-16.440 ± 0.928	9.529 ± 0.512	-1.052 ± 0.069
	14.5	2	-13.423 ± 0.794	5.550 ± 0.414	-0.581 ± 0.053
		3	-13.271 ± 1.018	6.172 ± 0.550	-0.634 ± 0.073
		4	-13.385 ± 1.252	6.738 ± 0.698	-0.669 ± 0.095
		5	-13.594 ± 1.477	7.27 ± 0.847	-0.691 ± 0.118
	60	2	-12.14 ± 0.859	4.606 ± 0.459	-0.448 ± 0.519
		3	-12.063 ± 1.054	5.270 ± 0.583	-0.507 ± 0.079
		4	-12.525 ± 1.283	6.022 ± 0.731	-0.567 ± 0.101
		5	-13.040 ± 1.516	6.72± 0.885	-0.611 ± 0.126

Table 5: Values of slope σ_q for the experimental and AMPT events at different energies.

		Energy (A GeV/c)		
Type of events	q	4.5	14.5	60
Expt.	2	0.515 ± 0.021	0.744 ± 0.050	0.937 ± 0.063
	3	0.707 ± 0.032	1.023 ± 0.079	1.314 ± 0.098
	4	0.950 ± 0.044	1.392 ± 0.116	1.682 ± 0.147
	5	1.228 ± 0.059	1.730 ± 0.158	2.103 ± 0.203
AMPT	2	0.488 ± 0.018	0.795 ± 0.045	0.808 ± 0.062
	3	0.637 ± 0.029	1.025 ± 0.076	1.158 ± 0.098
	4	0.833 ± 0.044	1.331 ± 0.118	1.429 ± 0.148
	5	1.061 ± 0.062	1.588 ± 0.170	1.754 ± 0.207

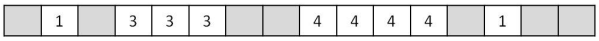

Fig. 1. Schematic representation of a typical void pattern in one dimensional space.

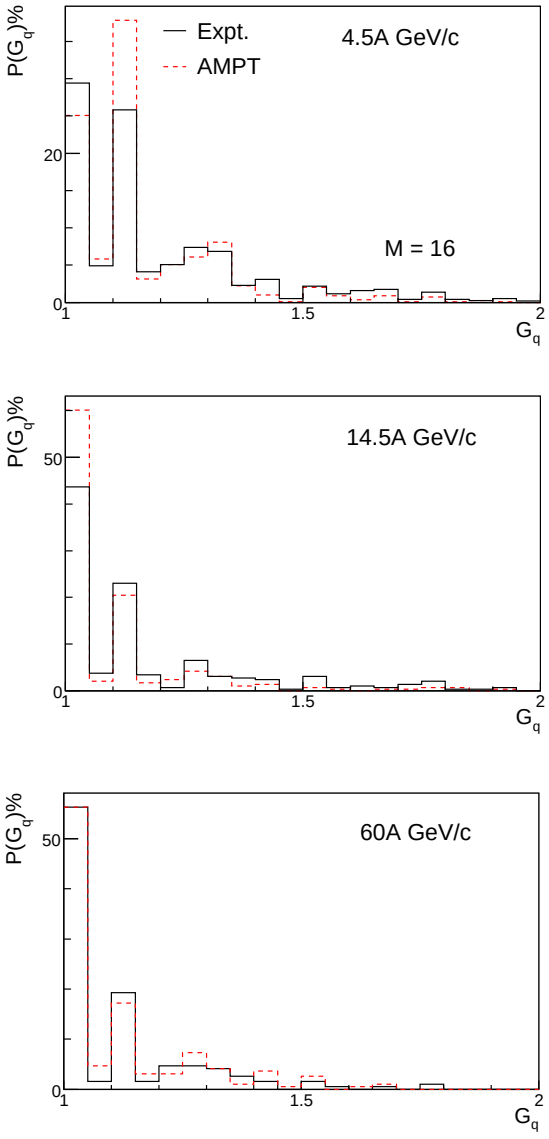

Fig. 2. G_q distributions for q =2 and M = 16 for the real and AMPT data on 4.5, 14.5 and 60A GEV/c ^{32}S-AgBr interactions.

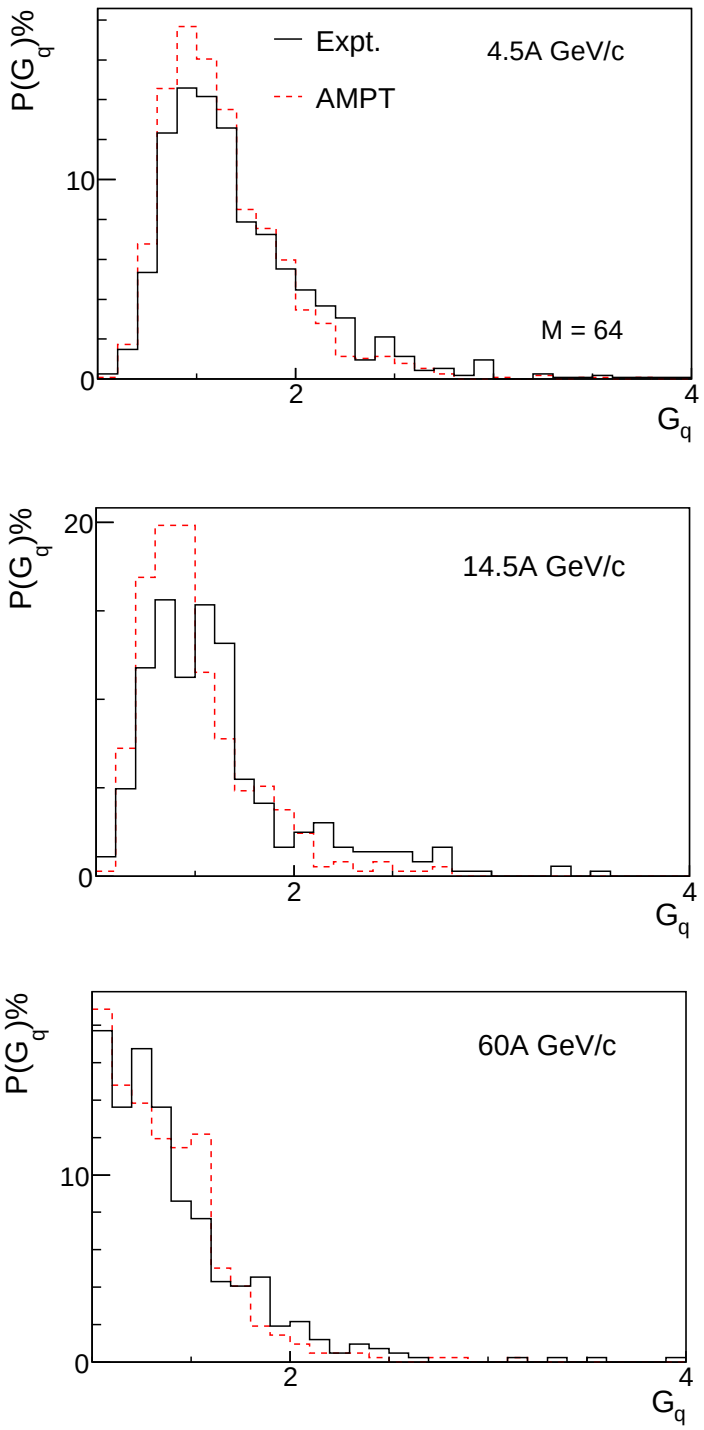

Fig. 3. G_q distributions for q = 2 and M = 64 for the experimental and AMPT data on 4.5, 14.5 and 60A GEV/c ^{32}S-AgBr collisions.

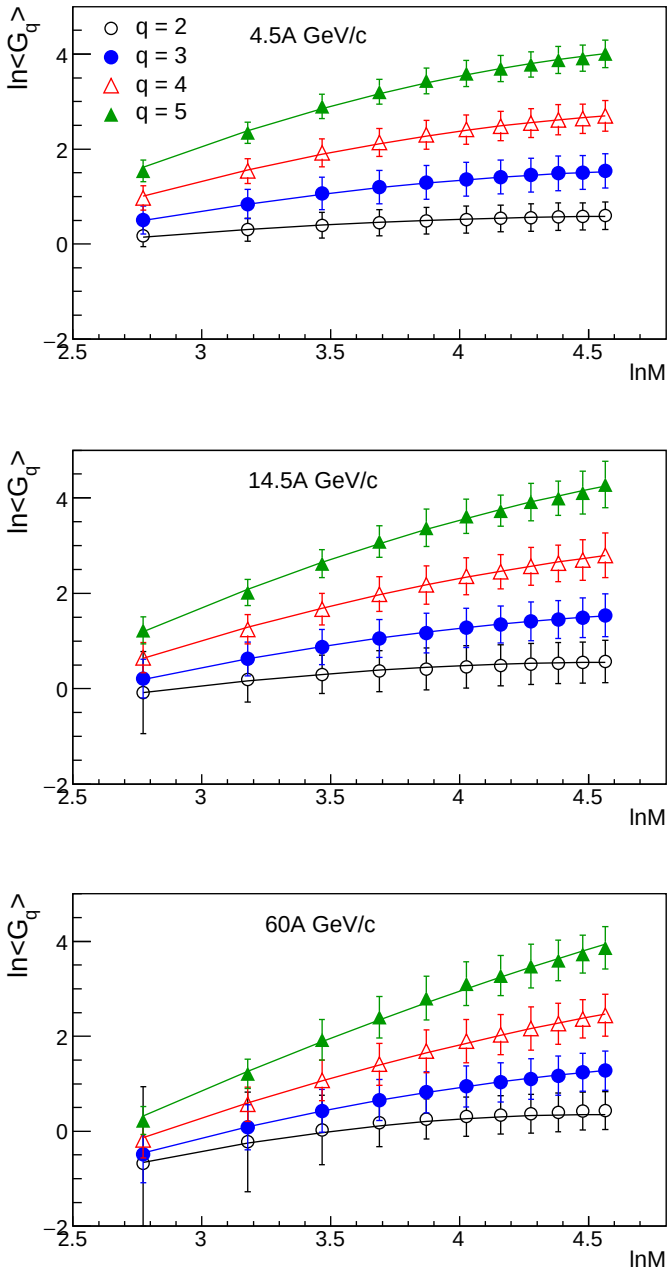

Fig. 4. Dependence of $ln < G_q >$ on lnM for the experimental events at the three incident energies.

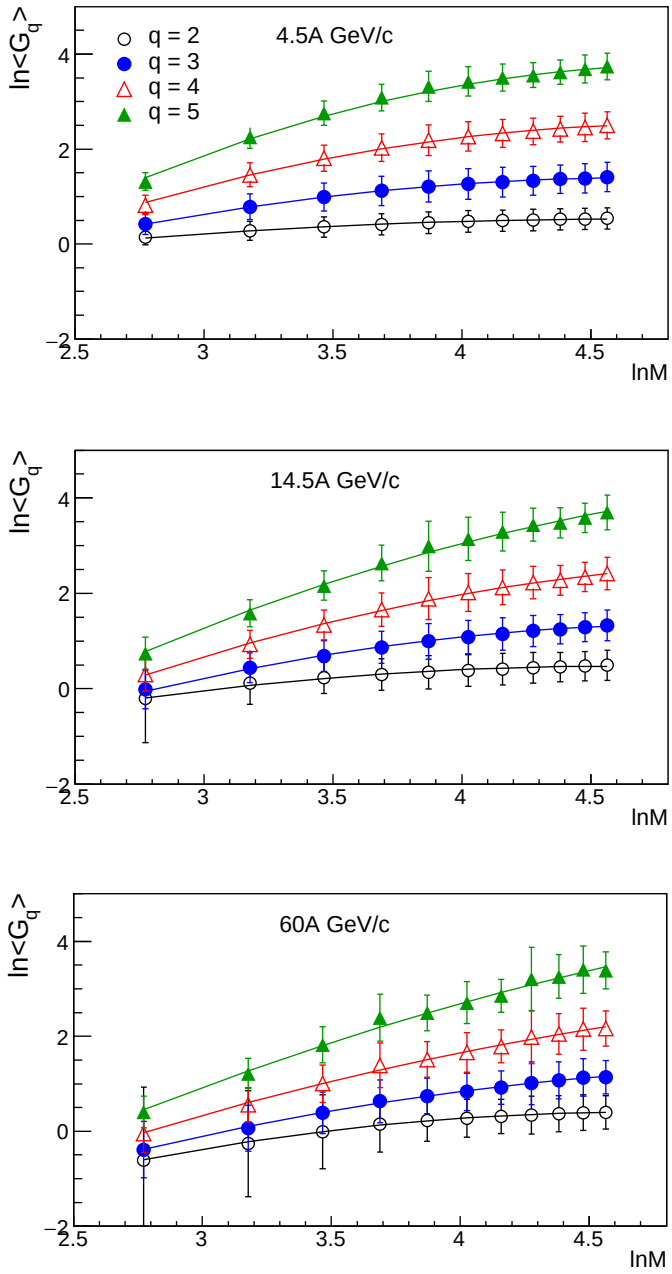

Fig. 5. Variations of $ln < G_q >$ with lnM for the AMPT generated events at the three incident energies.

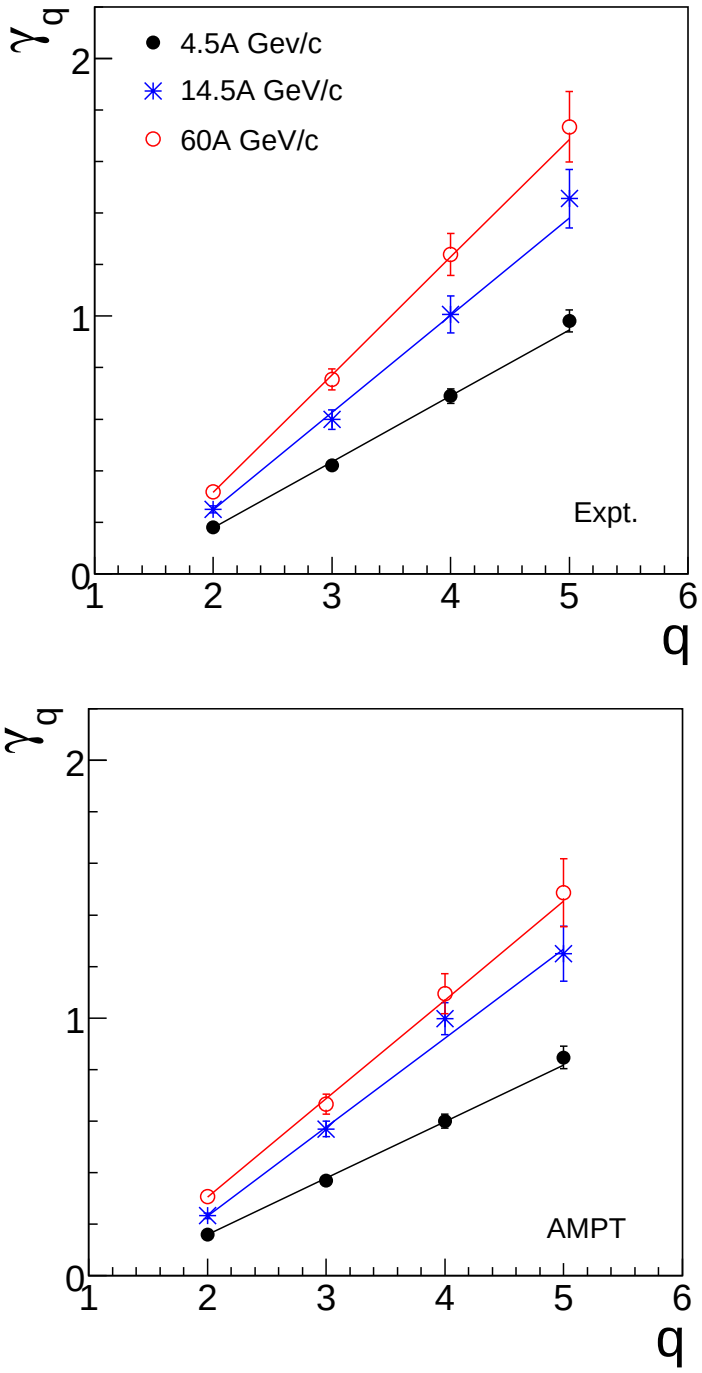

Fig. 6. Variations of γ_q with q for the experimental and AMPT simulated events at the three incident energies.

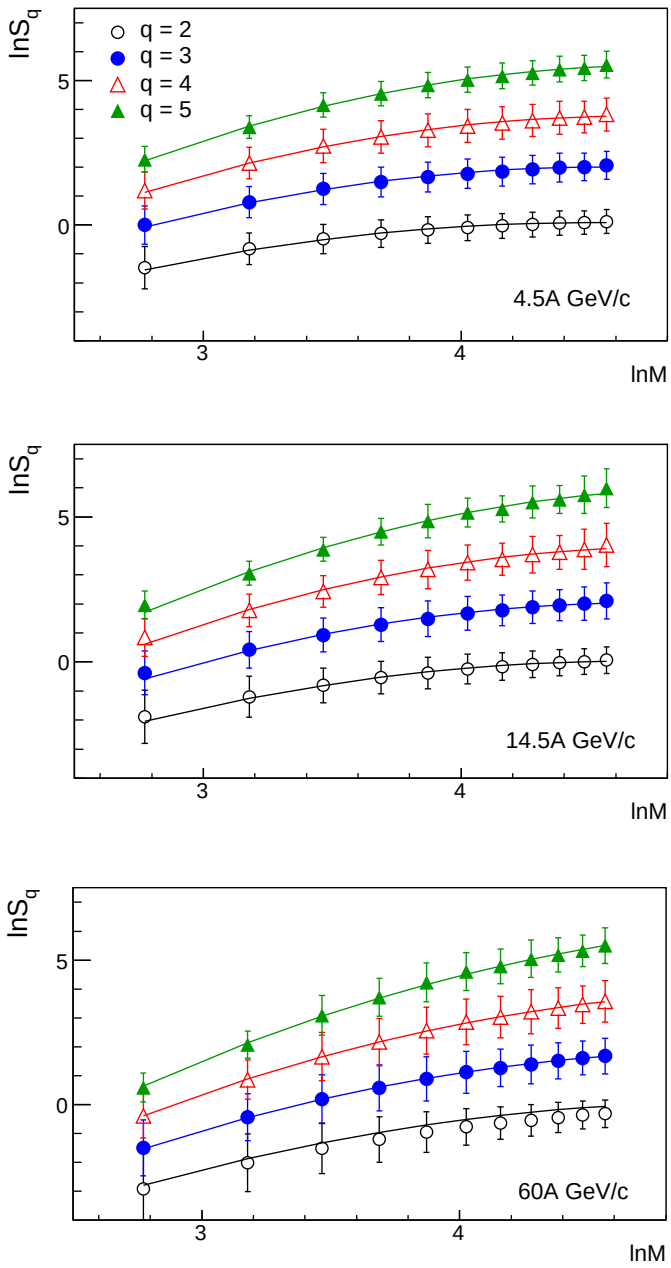

Fig. 7. Variations of lnS_q with lnM for the experimental 4.5, 14.5 and 60A GeV/c ^{32}S-AgBr interactions.

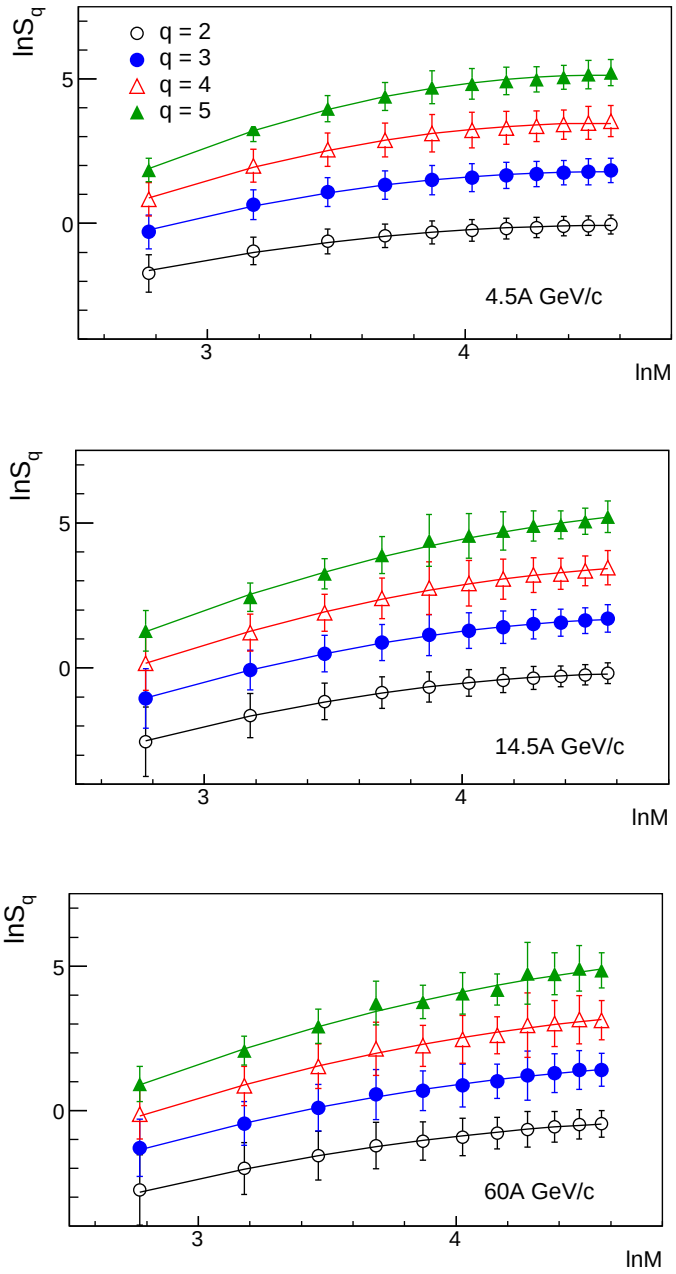

Fig. 8. Variations of lnS_q with lnM for the AMPT generated 4.5, 14.5 and 60A GeV/c ^{32}S-AgBr collisions.

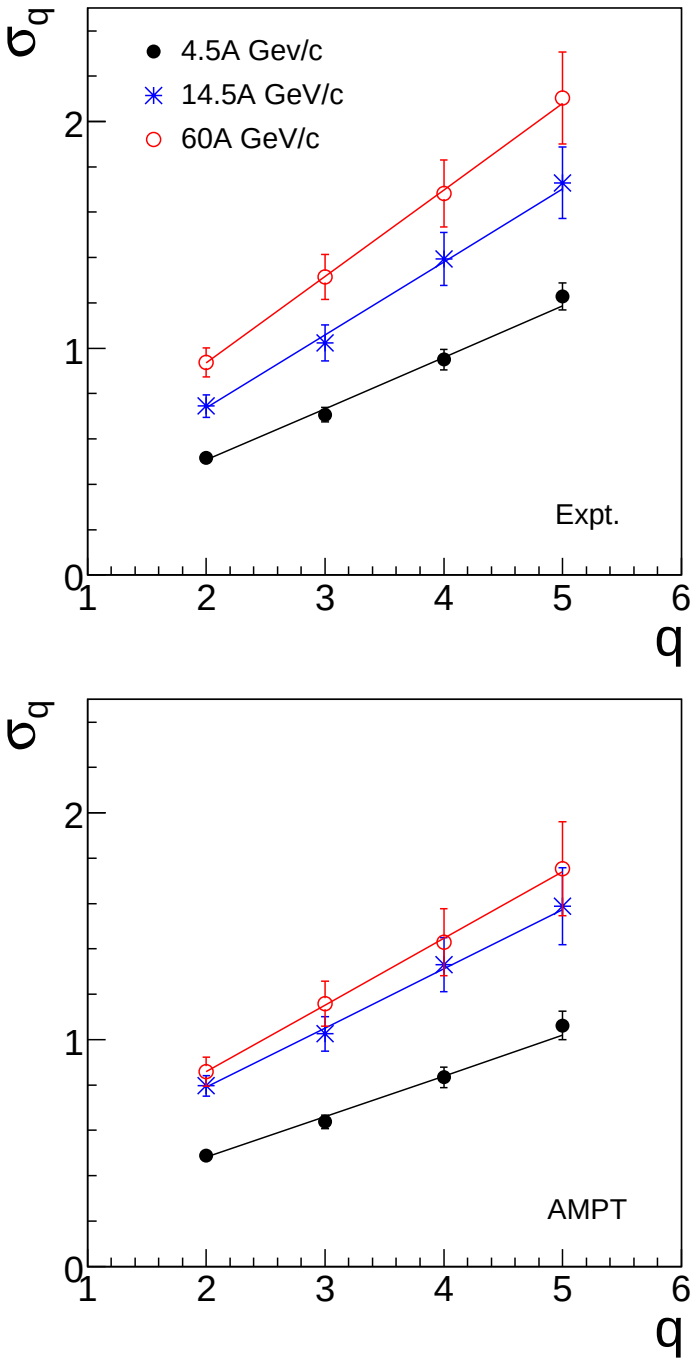

Fig. 9. Variations of σ_q with q for the experimental and AMPT events at the three incident energies.